NASA TECHNICAL NOTE

NASA TN D-4899

NASA TN D-4899

PREDICTION OF THERMODYNAMIC EFFECTS OF DEVELOPED CAVITATION BASED ON LIQUID-HYDROGEN AND FREON-114 DATA IN SCALED VENTURIS

by Royce D. Moore and Robert S. Ruggeri

Lewis Research Center
Cleveland, Ohio

NATIONAL AERONAUTICS AND SPACE ADMINISTRATION • WASHINGTON, D. C. • NOVEMBER 1968

NASA TN D-4899

PREDICTION OF THERMODYNAMIC EFFECTS OF DEVELOPED CAVITATION BASED ON LIQUID-HYDROGEN AND FREON-114 DATA IN SCALED VENTURIS

By Royce D. Moore and Robert S. Ruggeri

Lewis Research Center
Cleveland, Ohio

NATIONAL AERONAUTICS AND SPACE ADMINISTRATION

For sale by the Clearinghouse for Federal Scientific and Technical Information
Springfield, Virginia 22151 – CFSTI price $3.00

ABSTRACT

Cavity-pressure-depression measurements made in cavitated regions of hydrogen and Freon-114 (dichlorotetrafluoroethane) in two scaled venturis were used to evaluate experimental exponents of previously reported equations for the prediction of thermodynamic effects of cavitation for venturis. This prediction method accounts for changes in liquid, temperature, flow velocity, cavity length, and venturi scale. Use of the method requires similarity of body and cavity and a known cavity-pressure depression at one operating condition. The experimental data used included a velocity range of 20 to 205 feet per second (6.1 to 62.5 m/sec) and cavity lengths from 0.2 to 2.7 free-stream diameters.

PREDICTION OF THERMODYNAMIC EFFECTS OF DEVELOPED CAVITATION BASED ON LIQUID-HYDROGEN AND FREON-114 DATA IN SCALED VENTURIS

by Royce D. Moore and Robert S. Ruggeri

Lewis Research Center

SUMMARY

Cavity-pressure-depression measurements obtained from venturi tests with liquid hydrogen and Freon-114 (dichlorotetrafluoroethane) were used to evaluate experimental exponents of previously reported equations for the prediction of the thermodynamic effects of cavitation. This prediction method, which requires a known cavity-pressure depression at one operating condition, accounts for changes in liquid, liquid temperature, flow velocity, cavity length, and venturi scale. This method works well provided (1) there is local equilibrium of cavity temperature and pressure, and (2) the cavitated region is uniformly developed around the periphery of the venturi and its leading edge is at a fixed axial location. The pressure-depression data available for hydrogen in a 0.7-scale venturi covered a temperature range of 36.5° to 42.0° R (20.3 to 23.3 K), a flow velocity range of 110 to 205 feet per second (33.5 to 62.5 m/sec), and a cavity length of 1.0 to 2.6 free-stream diameters. The corresponding test ranges for Freon-114 in both a 0.7- and 1.0-scale venturi are 460° to 546° R (255.6 to 303.2 K), 20 to 50 feet per second (6.1 to 15.2 m/sec), and 0.2 to 2.7 free-stream diameters. A cavitation similarity parameter, which is based on minimum cavity pressure, was evaluated and shown to remain essentially constant for all conditions studied.

INTRODUCTION

Since cavitation is a vaporization process that involves heat and mass transfer, the physical properties of the liquid and its vapor, and the local temperature, pressure, and velocity, all affect the cavitation performance of hydraulic equipment. These combined effects of fluid properties, flow conditions, and heat transfer, termed thermodynamic effects of cavitation, can improve cavitation performance. For example, flow

devices such as venturis and pumps, operated under cavitating conditions in liquid hydrogen, butane, Freon, and hot water, will have lower inlet pressure requirements with respect to vapor pressure than when operated with cold water (refs. 1 to 9). This improvement (decrease) in inlet-pressure requirements results from the varying degrees of evaporative cooling associated with the cavitation process. This cooling lowers the pressure in the cavity which lowers, by a corresponding amount, the inlet-pressure requirements for a given performance level and set of operating conditions.

Venturi cavitation studies with Freon-114 (dichlorotetrafluoroethane), liquid nitrogen, and water show that thermodynamic effects of cavitation for a given venturi design can be predicted for a range of flow velocities, liquids, liquid temperatures, cavity lengths, and venturi scales (refs. 7 to 9). Equations for predicting these thermodynamic effects of cavitation (refs. 7 and 8) were developed based on Freon-114 cavitation results only, which showed relatively small thermodynamic effects of cavitation. Also, the Freon-114 data were limited to flow velocities less than 50 feet per second (15.2 m/sec).

Subsequent cavitation data (ref. 10), with liquid hydrogen in a venturi identical to that of reference 8, were obtained for a velocity range of 110 to 205 feet per second (33.5 to 62.5 m/sec). Thermodynamic effects of cavitation for liquid hydrogen were about 100 times greater than those for Freon-114. These unusually large effects are attributed to the unique physical properties of hydrogen and to the higher velocities studied. It is desirable to extend the range of application of the previously reported prediction equations (refs. 7 and 8) to include this wider range of liquid-hydrogen data.

The objective of this investigation was to incorporate results of the liquid-hydrogen studies into the evaluation of the experimental exponents of the prediction equations and thereby extend the range of flow conditions and fluid properties over which the equations can be applied. Cavitation data, available for both liquid hydrogen and Freon-114 in venturi flow, are used herein to evaluate the necessary experimental exponents involved in the prediction method. The Freon-114 data were obtained for both a 1.0- and 0.7-scale venturi, whereas liquid-hydrogen data were for a 0.7-scale venturi identical to that used in the Freon-114 studies. The liquid-hydrogen data were obtained from a NASA-sponsored study conducted at the National Bureau of Standards (ref. 10). Freon-114 data were obtained at the NASA Lewis Research Center (refs. 7 and 8).

APPARATUS REVIEW

Venturis

A sketch of the transparent-plastic venturis used is shown in figure 1. Detailed descriptions of the accurately scaled venturis are given in references 7 to 9. Briefly,

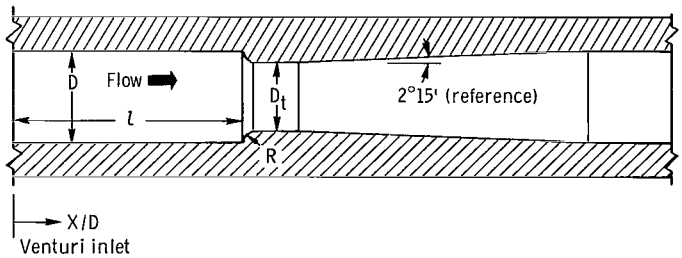

Free-stream diameter, D		Throat diameter, D_t		Approach section length, l		Radius of curvature, R	
in.	cm	in.	cm	in.	cm	in.	cm
1.0-Scale venturi							
1.743	4.43	1.377	3.50	4.198	10.66	0.183	0.465
0.7-Scale venturi							
1.232	3.13	0.976	2.48	2.964	7.53	0.128	0.325

Tap	Location, X/D	
	1.0-Scale venturi	0.7-Scale venturi
[a]1	1.98	1.81
2	2.49	----
3	2.52	2.53
4	2.62	2.61
5	----	2.71
6	2.83	2.84
7	3.02	3.01
8	3.30	3.30
9	3.73	3.73
10	4.31	4.32
11	4.88	4.88

[a]Free-stream static pressure location.

Figure 1. - Venturi test sections and location of instrumentation.

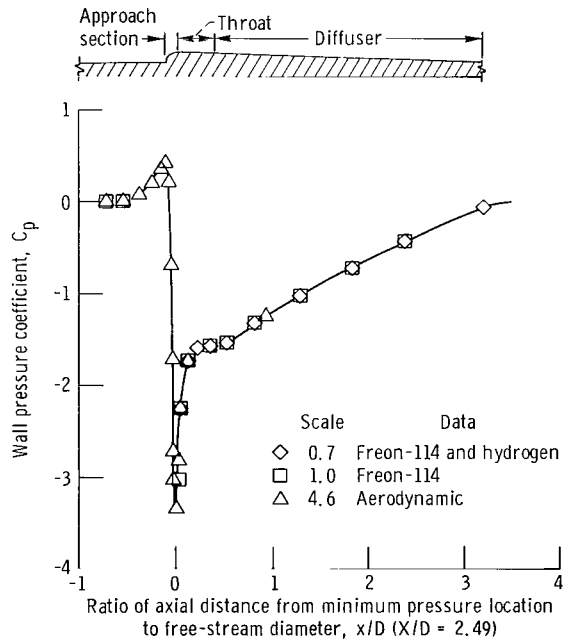

Figure 2. - Wall pressure distribution for venturis.

the venturis used a circular arc to provide convergence from the approach section to a constant-diameter throat section. The throat section is followed by a conical diffuser. The venturi that has the 1.743-inch (4.43-cm) free-stream diameter is referred to herein as the 1.0-scale venturi, and that with a 1.232-inch (3.13-cm) free-stream diameter is termed the 0.7-scale venturi. Both the 1.0- and 0.7-scale venturis were used for the Freon-114 tests. A 0.7-scale venturi was used for the liquid-hydrogen studies. The wall pressure distribution for these venturis is shown in figure 2.

Facilities

The NASA facility consists of a small closed-return hydrodynamic tunnel which was designed to circulate various liquids by a centrifugal pump. The tunnel, which is described in detail in references 9 and 11, had a capacity of 10 gallons (37.8 liters). The liquid-hydrogen test facility used by NBS (ref. 10) consisted of a blowdown system with the test section located between the supply and receiver Dewars. The capacity of the Dewars was 265 gallons (1000 liters). Times available for steady-state data acquisition in the NBS facility ranged from about 20 to 40 seconds.

Instrumentation

In the NASA facility, the free-stream static pressures were measured by calibrated precision gages. The pressures within the cavitated regions were measured by a multiple-tube mercury manometer. The free-stream liquid temperature was determined by a calibrated copper-constantan thermocouple. The temperatures within the cavitated region were measured as a difference between the free-stream temperature and the local cavity temperature by calibrated copper-constantan thermocouples. The thermocouples used to measure cavity temperature were mounted flush with, but did not contact, the venturi walls (see ref. 7).

In the liquid-hydrogen facility (ref. 10), the pressure measurements were obtained with calibrated pressure transducers. The free-stream liquid temperature was measured with a platinum resistance thermometer. Calibrated Chromel-constantan thermocouples were used to determine temperatures within the cavitated region. As in the Freon-114 studies, the thermocouple circuit was designed to read the temperature difference between local-cavity and the upstream-reference temperatures. These wall thermocouples were flush-mounted in the same way as those used for the Freon-114 studies. The estimated overall accuracies of the measurements and readout systems are listed in table I.

TABLE I. - RANGE AND ESTIMATED OVERALL ACCURACY OF

MEASUREMENT AND READOUT SYSTEM

(a) Liquid hydrogen

Measurement	Range	Accuracy
Free-stream static pressure, h_0, ft of liquid; m of liquid	750 to 2000; 228.7 to 600	±2.0 percent
Minimum cavity pressure, $h_{c,min}$, ft of liquid; m of liquid	250 to 1000; 76.2 to 304.8	±2.0 percent
Free-stream liquid temperature, T, ^{o}R; K	36.5 to 42.0; 20.3 to 23.3	±0.1^{o} R; ±0.1 K
Temperature depression at leading edge of cavity, Δt, ^{o}R; K	2.6 to 5.6; 1.4 to 3.1	[a]±1.0^{o} R; ±0.6 K

(b) Freon-114

Measurement	Range	Accuracy
Free-stream static pressure, h_0, ft of liquid; m of liquid	20 to 150; 6.0 to 45.7	±1.0 percent
Minimum cavity pressure, $h_{c,min}$, ft of liquid; m of liquid	7.5 to 48.0; 2.3 to 14.6	±0.2 percent
Free-stream liquid temperature, T, ^{o}R; K	460 to 546; 255.6 to 303.2	±0.2^{o} R; ±0.1 K
Temperature depression at leading edge of cavity, Δt, ^{o}R; K	0.6 to 10.5; 0.3 to 5.8	[b]±0.2^{o} R; ±0.1 K

[a]Equivalent to about ±100 ft at 36.5^{o} R and ±160 ft at 42.0^{o} R or ±30.5 m at 20.3 K and ±48.8 m at 23.3 K.

[b]Equivalent to about ±0.05 ft at 460^{o} R and ±0.3 ft at 546^{o} R or ±0.02 m at 255.6 K and ±0.1 m at 303.2 K).

ANALYTICAL REVIEW

A simple heat balance at the vapor-liquid interface of the cavitated region is reviewed first followed by a method for estimating the volume ratio term in the heat-balance equation. Then a cavitation similarity parameter that accounts for the thermodynamic effects of cavitation is reviewed.

Heat Balance

The temperature depressions measured within a cavitated region are attributed to cooling of the liquid along the vapor-liquid interface because the heat required for vapor-

ization is drawn from a thin layer of adjacent liquid. If the vapor in the cavity is locally in equilibrium with the liquid of the cooled layer and there are no partial pressures of permanent gases, the local cavity pressure will drop to the vapor pressure corresponding to the reduced local temperature. The vapor-pressure depression is a function of the physical properties of the fluid, body geometry, velocity, and the heat- and mass-transfer mechanisms involved. The magnitude of the local cavity-pressure depression can be estimated through a heat balance between the heat required for vaporization and the heat drawn from the adjacent liquid. This heat-balance analysis is presented in reference 7.

From the heat-balance analysis, the vapor-pressure depression Δh_v is expressed as a function of vapor- to liquid-volume ratio. This relation is plotted in figure 3 for liquid hydrogen and Freon-114. The liquid volume in this ratio is only that which is involved in the vaporization process and is only a small fraction of the entire liquid stream. As shown in reference 7, a useful and close approximation of the curves of figure 3 may be obtained from the expression

$$\Delta h_v \cong J\left[\left(\frac{\rho_v}{\rho_l}\right)^2\left(\frac{L^2}{c_l T}\right)\left(\frac{\forall_v}{\forall_l}\right)\right] \tag{1}$$

(All symbols are defined in the appendix.) Local equilibrium of the vapor and liquid phases is assumed for the derivation of equation (1) or for the curves of figure 3.

The vapor- to liquid-volume ratio $\forall_v/\forall_l$ for the experimental case is not known or measured directly, and thus the values of this ratio from figure 3 are used only in a relative sense. Useful predictions have been made by determining an effective or reference value of $\forall_v/\forall_l$ from measured cavity-pressure depressions Δh_v for one model scale, liquid, temperature, velocity, and cavity length. Then values of $\forall_v/\forall_l$ for other model scales, liquids, temperatures, velocities, and cavity lengths are estimated, as described subsequently, relative to this reference value. With these predicted $\forall_v/\forall_l$ values and figure 3, determination of Δh_v values, relative to reference data, is possible.

Estimation of Vapor- to Liquid-Volume Ratio

It is shown in reference 7 that for one venturi scale, the vapor- to liquid-volume ratio can be predicted, relative to a reference value of $\forall_v/\forall_l$, for changes in liquid, temperature, velocity, or cavity length. Subsequent venturi cavitation studies with different venturi scales (ref. 8) have shown that, for a constant scaled cavity length ($\Delta x/D$ = constant), the value of volume ratio for a scaled model, relative to the prototype,

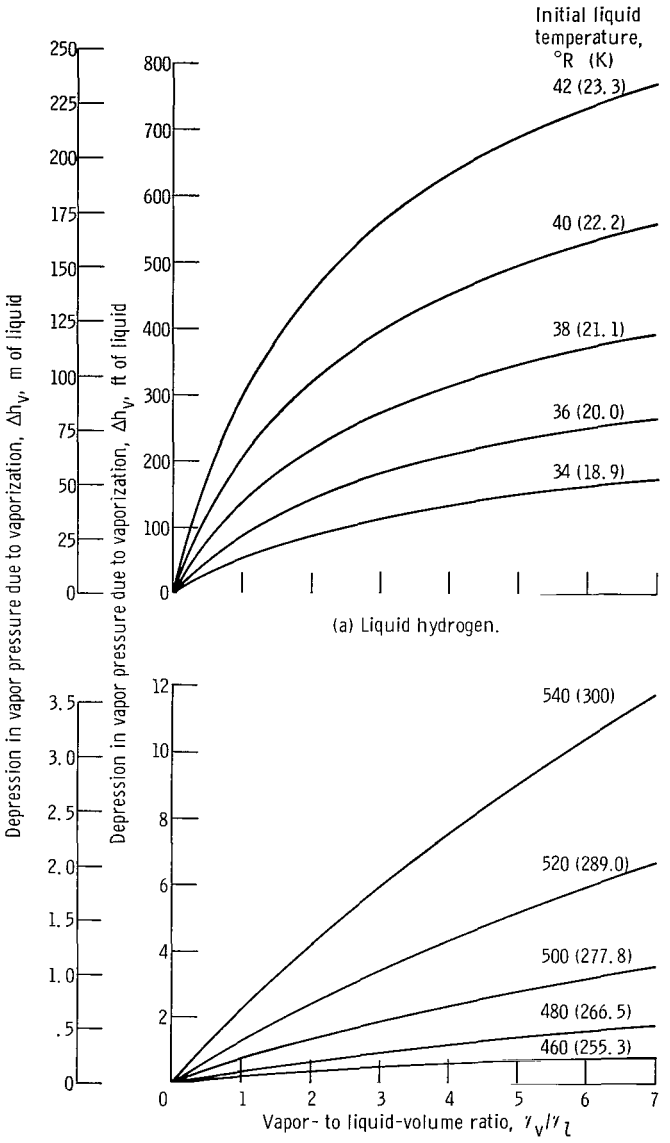

Figure 3. - Vapor-pressure depression as function of amount of liquid vaporized.

can also be predicted. Combining the prediction equations of references 7 and 8 yields the following general equation for predicting the vapor- to liquid-volume ratio, relative to a reference value, for changes in liquid, liquid temperature, flow velocity, cavity length, and venturi scale:

$$\left(\frac{\rho_v}{\rho_l}\right)_{pred} = \left(\frac{\rho_v}{\rho_l}\right)_{ref} \left(\frac{\alpha_{ref}}{\alpha}\right)^m \left(\frac{V_0}{V_{0,ref}}\right)^n \left(\frac{D}{D_{ref}}\right)^{1-n} \left[\frac{\frac{\Delta x}{D}}{\left(\frac{\Delta x}{D}\right)_{ref}}\right]^p \tag{2}$$

The exponents m, n, and p depend on the heat-transfer process involved and must be experimentally determined. Since these exponents will now be based on both liquid-hydrogen and Freon-114 data, which cover a much wider range of flow conditions and fluid properties than that previously used in references 7 and 8, the resulting equation would have a greater range of application. The derivation and use of equation (2) requires the cavitated region to be uniformly developed around the periphery of the venturi and the leading edge of this cavitated region to be at a fixed axial location.

Cavitation Similarity Parameters

The conventional cavitation parameter is usually expressed as

$$K_v \equiv \frac{h_0 - h_v}{\frac{V_0^2}{2g}} \tag{3}$$

The parameter K_v for developed cavitation is derived from the assumption that Bernoulli's equation for steady ideal flow applies between a free-stream location and the cavity surface and that the cavity surface is at a constant pressure equal to free-stream vapor pressure. However, because of the previously discussed thermodynamic effects of cavitation, the cavity pressure can be significantly less than free-stream vapor pressure and can also vary with axial distance. Thus, a more general expression for the cavitation parameter would have h_v in equation (3) replaced with a more appropriate reference pressure in the cavity. As in references 7 and 8, the minimum measured cavity pressure (which corresponds to the maximum cavity-pressure depression) is selected as the reference pressure to define the following developed cavitation parameter:

$$K_{c,min} = \frac{h_0 - h_{c,min}}{\frac{V_0^2}{2g}} = \frac{h_0 - h_v}{\frac{V_0^2}{2g}} + \frac{\Delta h_v}{\frac{V_0^2}{2g}} = K_v + \frac{\Delta h_v}{\frac{V_0^2}{2g}} \quad (4)$$

The venturi cavitation studies of references 7 and 8 show that $K_{c,min}$ is approximately constant over the range of liquids, temperatures, velocities, and venturi scales tested, provided that the geometric similarity of the cavitated region is maintained. Cavities are considered to have geometric similarity when they have uniform peripheral development with the cavity leading edge at a fixed axial location and have a constant value of $\Delta x/D$. It has been observed that when the leading edge of the cavitated region becomes erratic and ill-defined, $K_{c,min}$ does not remain constant (see ref. 7). In general, it is not possible to predict which conditions of liquid, temperature, velocity, or scale will result in a nonuniform or erratic cavitated region.

For the range of conditions reported herein, the appearance of hydrogen cavitation in the 0.7-scale venturi was similar to that of Freon-114 in both the 0.7- and 1.0-scale venturis. Photographs of typical cavitation in both liquids are shown in figure 4. Although vapor formations in hydrogen are more homogeneous, the cavitated region in both liquids is composed of many individual vapor streamers uniformly developed around the periphery of the venturi. These streamers merge within a few millimeters to form a thin annulus of a frothy and turbulent vapor-droplet mixture adjacent to the wall. The leading edge of these streamers remains fixed at or near the minimum-pressure location. Within the venturi throat, the nominal thickness of the cavitated region is estimated to be between 0.01 and 0.03 inch (0.03 and 0.08 cm) although direct measurements were not made. Because the cavities exhibit a uniform peripheral development with their leading edge at a fixed axial location, the data obtained for both hydrogen and Freon-114 are considered equally valid in the determination of $K_{c,min}$.

For constant values of $K_{c,min}$ and V_0 in equation (4), a change in Δh_v results in a corresponding change in $h_0 - h_v$. This pressure difference $h_0 - h_v$ is a measure of free-stream pressure requirements to obtain geometrically similar cavities and includes the thermodynamic effects of cavitation. Thus, for the wide range of conditions for which $K_{c,min}$ is constant, it is a most useful cavitation similarity parameter. When at least one value of Δh_v (or $h_{c,min}$) is known and used as the reference value for predicting other values of Δh_v, as previously discussed, the free-stream pressure requirements for untested conditions can be predicted by equation (4).

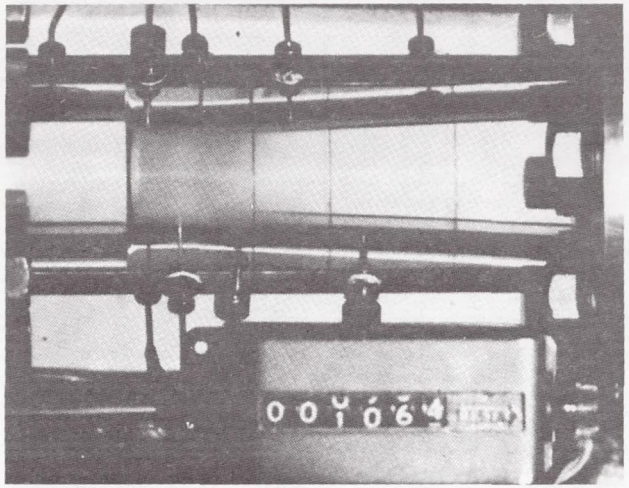

(a) Liquid hydrogen in 0.7-scale venturi; nominal cavity length, 1.0 free-stream diameter.

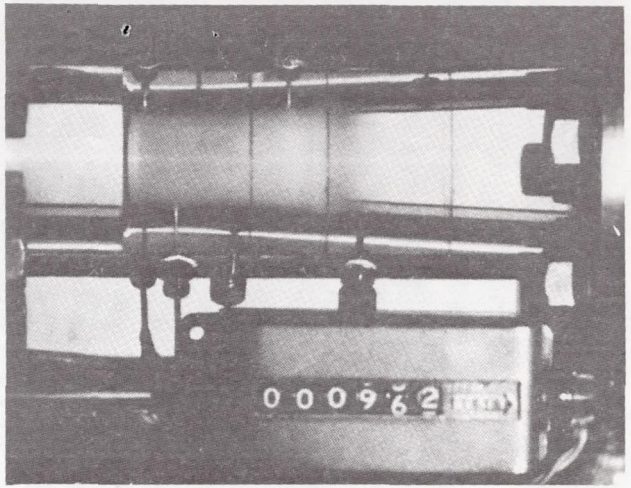

(b) Liquid hydrogen in 0.7-scale venturi; nominal cavity length, 1.6 free-stream diameters.

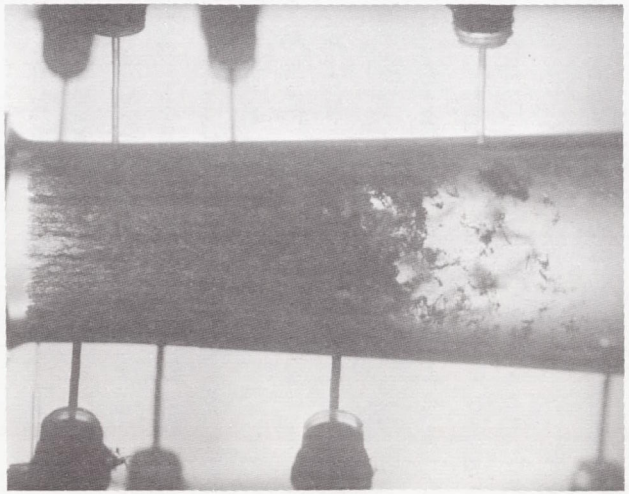

(c) Freon-114 in 0.7-scale venturi; nominal cavity length, 1.4 free-stream diameters.

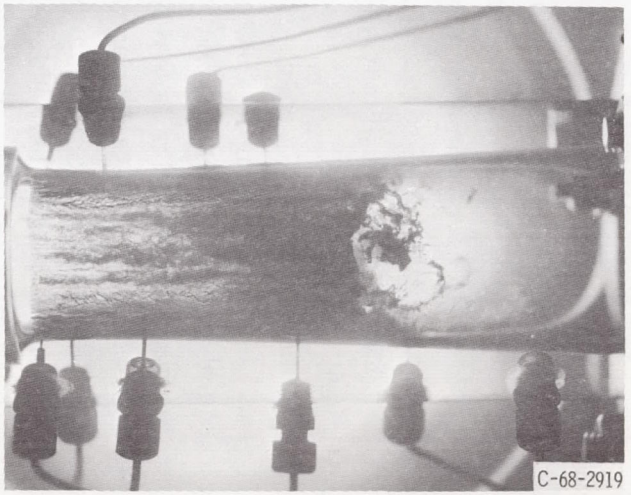

(d) Freon-114 in 1.0-scale venturi; nominal cavity length, 1.5 free-stream diameters.

Figure 4. - Typical cavitation in venturis.

RESULTS AND DISCUSSION

Typical experimental cavity-pressure depressions obtained for liquid hydrogen in the 0.7-scale venturi (taken from ref. 10) are discussed first, followed by a brief discussion of Freon-114 results obtained in both the 0.7- and 1.0-scale venturis (refs. 7 and 8). The exponents of the prediction equation are then evaluated. A brief discussion of the developed cavitation similarity parameter $K_{c,min}$ is also presented.

Liquid-Hydrogen Results

For the cavitation studies in liquid hydrogen (ref. 10), the free-stream velocity was varied from 110 to 205 feet per second (33.5 to 62.5 m/sec) at controlled temperatures from 36.5° to 42.0° R (20.3 to 23.3 K). The cavity length was varied from 1.0 to 2.6 free-stream diameters.

As expected from the curves for vapor- to liquid-volume ratio in figure 3(a), local measured pressures within cavitated regions of liquid hydrogen were considerably less than free-stream vapor pressure. The lowest measured pressure occurs in the upstream portion of the cavity, usually at or near the leading edge. Cavity pressure then increases with axial distance reaching stream vapor pressure at the cavity trailing edge. Maximum cavity-pressure depressions below free-stream vapor pressure ranged from 185

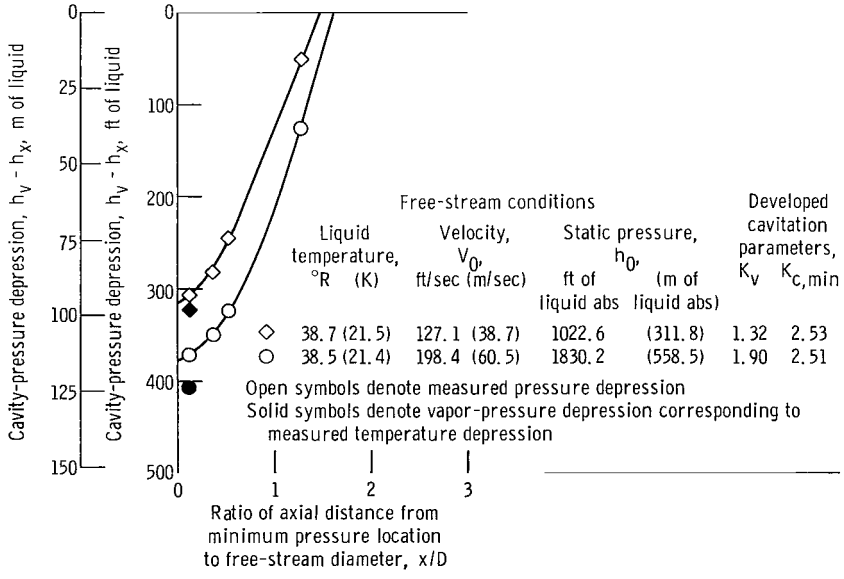

Figure 5. - Effect of free-stream velocity on pressure depression within cavitated hydrogen region for nominal cavity length of 1.5 free-stream diameters in 0.7-scale venturi.

feet of liquid (56.4 m of liquid) at the low-velocity low-temperature condition to 580 feet of liquid (177 m of liquid) at the higher flow velocities and temperatures studied.

Specific trends in cavity-pressure depressions with regard to free-stream velocity, liquid temperature, and cavity length are shown in figures 5, 6, and 7, respectively. Cavity-pressure depression is plotted as a function of the ratio of axial distance from minimum-pressure location to the free-stream diameter. The measured temperature depression in the leading-edge region of the cavity was converted to its corresponding vapor-pressure depression by use of the vapor-pressure - temperature curve. These points are also shown in figures 5 to 7.

An increase in free-stream velocity results in an increase in the cavity-pressure depression. This effect is shown in figure 5 for a hydrogen temperature of about 38.7° R (21.5 K) and it is typical of all temperatures studied.

An increase in the liquid temperature results in an increase in cavity-pressure depression (fig. 6). This trend was observed for each velocity tested.

As the cavity length was increased, the cavity-pressure depression increased over the full axial length of the cavity, as shown in figure 7. This trend was evident at all free-stream velocities and liquid temperatures studied.

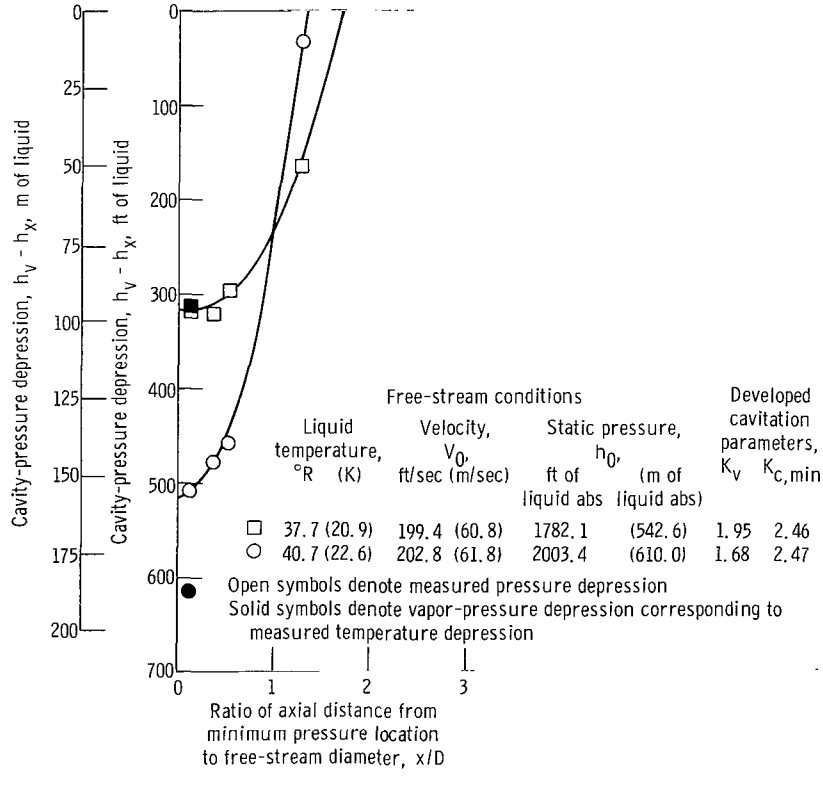

Figure 6. - Effect of free-stream liquid temperature on pressure depression within cavitated hydrogen region for nominal cavity length of 1.5 free-stream diameters in 0.7-scale venturi.

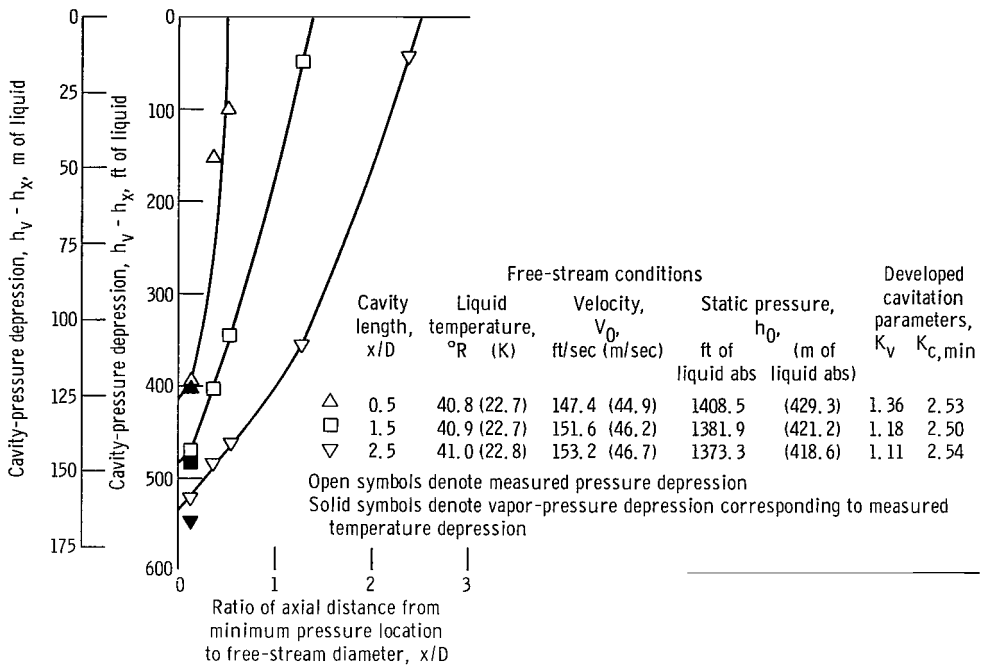

Figure 7. - Effect of cavity length on pressure depression within cavitated hydrogen region in 0.7-scale venturi.

At the leading edge of the cavity, the vapor-pressure depressions corresponding to the measured temperature depressions were not always in agreement (i.e., in equilibrium) with the measured cavity-pressure depressions. For example, in figure 6, agreement is shown for the 37.7° R (20.9 K) data, while for the 40.7° R (22.6 K) data the measured cavity-pressure depression is about 100 feet of liquid (30.5 m of liquid) less than the vapor-pressure depression. The difference between cavity-pressure depression and vapor-pressure depression is, however, within the accuracy of the temperature depression measurement (see footnote a of table I). The extent to which equilibrium conditions existed near the leading edge of the cavity could not, therefore, be determined.

Freon-114 Results

For the Freon-114 cavitation investigation in both the 0.7- and 1.0-scale venturis (refs. 7 and 8), the free-stream velocity was varied from 19 to 50 feet per second (5.8 to 15.2 m/sec) at controlled temperatures from 460° to 546° R (255.6 to 303.2 K). The cavity lengths were varied from 0.2 to 2.7 free-stream diameters.

Cavity-pressure depressions for Freon-114 in both the 0.7- and 1.0-scale venturis showed the same trends as liquid hydrogen with respect to free-stream velocity, liquid temperature, and cavity length. However, the cavity-pressure depressions were much

smaller for Freon-114 and ranged from 0.5 to 11.0 feet of liquid (0.2 to 3.4 m of liquid) depending on flow conditions and temperature. As with hydrogen, the maximum cavity-pressure depression occurred at the leading edge of the cavity. Good agreement between measured cavity-pressure depressions and depressions based on locally measured temperatures resulted for all the Freon-114 tests in both venturis. Thus, for engineering purposes, a condition of local equilibrium existed at the vapor-liquid interface for all Freon-114 cavities studied.

Evaluation of Exponents

In all instances, the maximum measured cavity-pressure depressions were used to evaluate the exponents for the prediction equation (eq. (2)). All the Freon-114 data obtained in both the 0.7- and 1.0-scale venturis (refs. 7 and 8) were used. Because the analysis is based on conditions of thermodynamic equilibrium, only that portion of the liquid-hydrogen data which showed less than a 10-percent variation between measured cavity-pressure depression and vapor-pressure depression corresponding to measured temperature depression was used. These Freon-114 and hydrogen data were used in conjunction with the method of least squares (ref. 12) to solve for all the exponents simultaneously. More than 100 data points were used. The resulting values for the exponents are $m = 1.0$, $n = 0.8$, and $p = 0.3$. Thus, equation (2) can be rewritten with the appropriate values for the exponents as

$$\left(\frac{\gamma_v}{\gamma_l}\right)_{pred} = \left(\frac{\gamma_v}{\gamma_l}\right)_{ref} \left(\frac{\alpha_{ref}}{\alpha}\right)^{1.0} \left(\frac{V_0}{V_{0,ref}}\right)^{0.8} \left(\frac{D}{D_{ref}}\right)^{0.2} \left[\frac{\frac{\Delta x}{D}}{\left(\frac{\Delta x}{D}\right)_{ref}}\right]^{0.3} \tag{5}$$

Except for the thermal diffusivity term, the exponents changed only slightly from those previously reported, which were $m = 0.5$, $n = 0.85$, and $p = 0.16$. In previous studies, the exponent on the thermal diffusivity term was based on the 25-percent change in thermal diffusivity over the experimental range in temperature for Freon-114. The present study, including the hydrogen results, covers 400-percent change in thermal diffusivity. Because equation (5) is based on a wider range of variables, it is preferred to the prediction equations previously reported.

The use of equation (5) instead of the original equation (ref. 7) has little effect on the results reported in previous studies (refs. 2, 3, 7, and 8) because of the small thermal-diffusivity ranges previously studied.

The agreement to be expected between experimental and predicted results is presented in figure 8. The complete test range of Δh_v is presented in figure 8(a), which

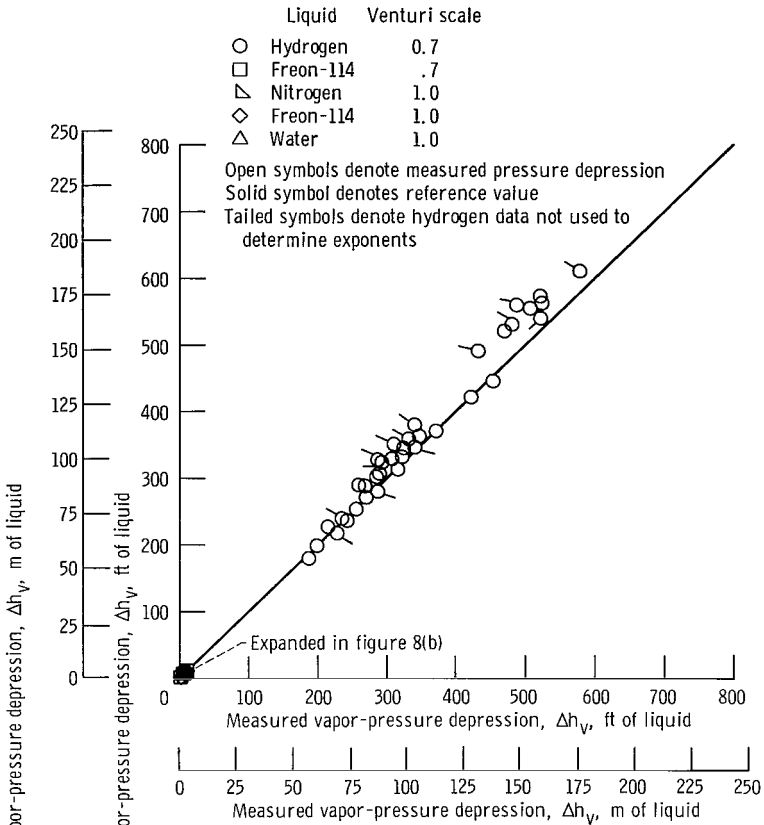

(a) Complete range of vapor-pressure depression.

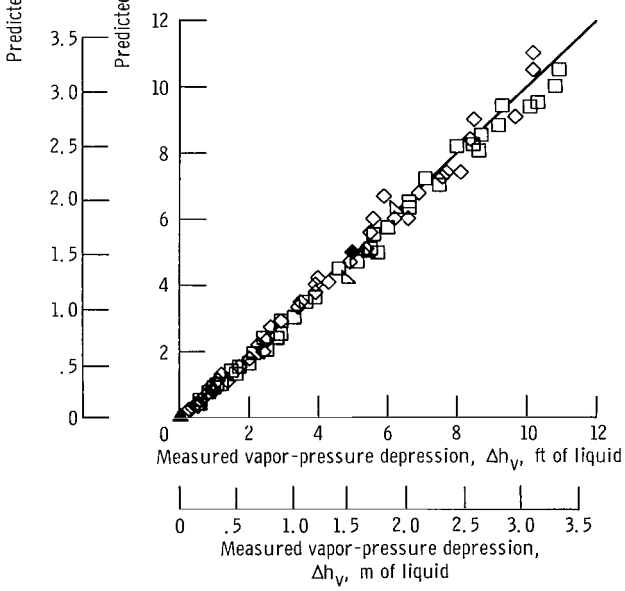

(b) Low range of vapor-pressure depressions.

Figure 8. - Comparison of measured and predicted vapor-pressure depressions.

emphasizes liquid-hydrogen data. The low range of vapor-pressure depressions is presented in figure 8(b).

The liquid-hydrogen data used in the evaluation of the exponents are shown as the untailed symbols in figure 8(a). For the remainder of the hydrogen data shown (tailed symbols), there were differences of between 10 and 22 percent in measured cavity-pressure depression and vapor-pressure depression corresponding to measured temperature depression. As previously indicated, it is not known if this second set of data (tailed symbols) is in equilibrium or not. However, comparing measured Δh_v with predicted Δh_v (fig. 8(a)), shows no significant difference in the two sets (tailed or untailed) of data.

Freon-114 data obtained in both venturis as well as available liquid-nitrogen and water data obtained in the 1.0-scale venturi are shown in figure 8(b). All points shown in figure 8 are based on a single reference value represented by the solid symbol. The reference value used was

Liquid	Freon-114
Venturi scale	1.0
Temperature, T, ^{o}R; K	538; 299
Free-stream velocity, V_0, ft/sec; m/sec	19.6; 6.0
Cavity length, $\Delta x/D$	0.72
Thermal diffusivity, ft^2/hr; m^2/hr	1.52×10^{-3}; 1.41×10^{-4}

The measured $\left(\Delta h_v\right)_{ref}$ is 5.0 feet of liquid (1.5 m of liquid). From figure 3(b), the corresponding $\left(\gamma_v/\gamma_l\right)_{ref}$ is 2.6. Predicted values of γ_v/γ_l were then calculated from equation (5) and the corresponding values of Δh_v appears to be quite good, considering the predicted values of up to 600 feet of liquid (183 m of liquid) were based on the single Freon-114 reference Δh_v value of 5 feet of liquid (1.5 m of liquid). This reference value was chosen because it represented the lowest velocity and thermal diffusivity values of this study. The selection of the reference value in equation (5) is, of course, arbitrary. However, regardless of the values selected, the difference between predicted and measured Δh_v values would have been less than 20 percent for the data of figure 8.

It is concluded that the simple analysis with the experimentally derived exponents can be useful in predicting cavity-pressure depressions with reasonably good accuracy over a wide range of fluid properties and flow conditions, provided that (1) maximum cavity-pressure depression is known for at least one operating condition, (2) there is a uniformly developed cavitated region with its leading edge at a fixed axial location, and (3) local equilibrium of temperature and pressure exists at the vapor-liquid interface.

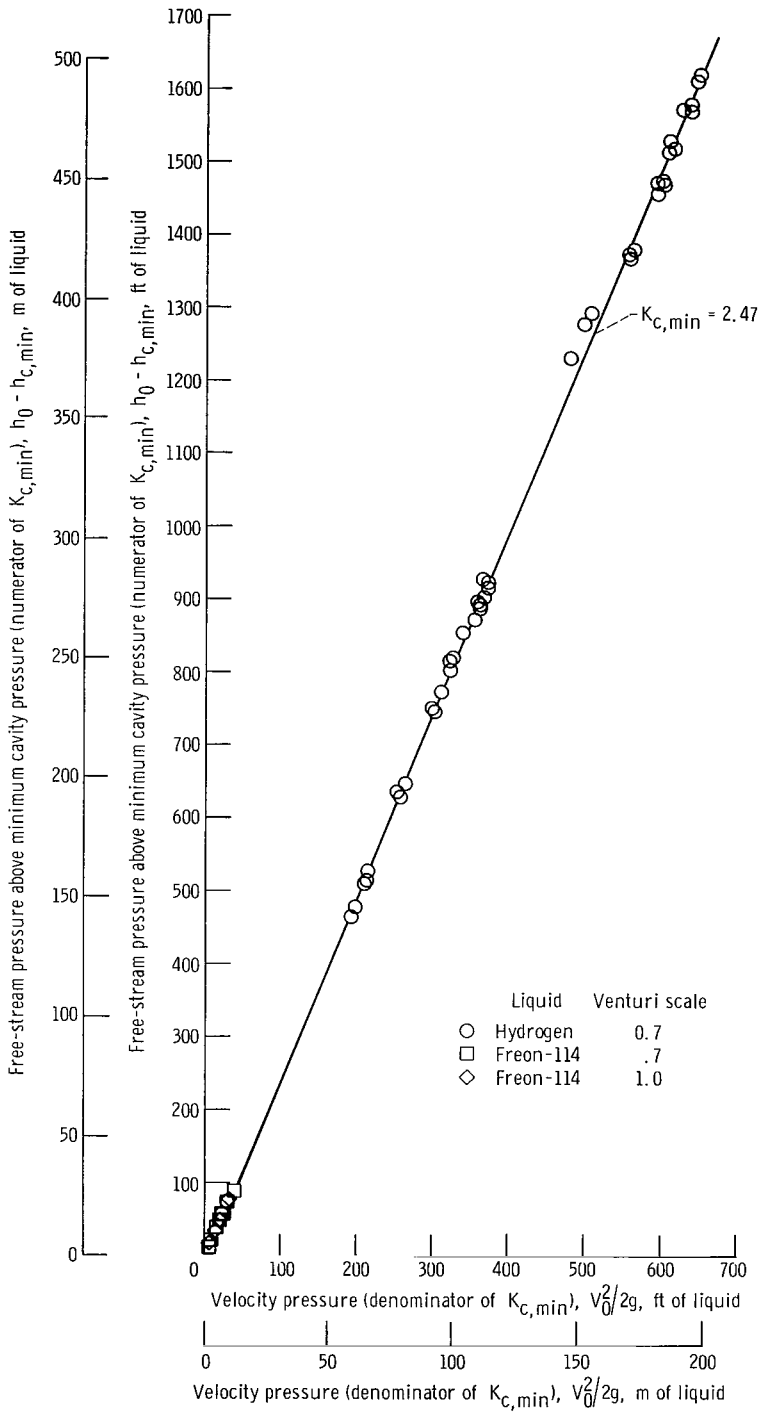

Figure 9. - Effects of venturi scale and liquid on minimum pressure of cavitated region.

Evaluation of Cavitation Parameter

The degree to which a constant value can be used to represent $K_{c,min}$ is shown graphically in figure 9, where the numerator of $K_{c,min}$ is plotted as a function of its denominator. The line shown is for a $K_{c,min}$ of 2.47. The good agreement between the data and the line indicates that a single $K_{c,min}$ value of 2.47 can be utilized to represent all the hydrogen and Freon-114 data. Although the value of $K_{c,min}$ remained constant for different cavity lengths, it is possible that for other venturi shapes $K_{c,min}$ will vary with cavity length.

Determination of Vapor-Pressure Depression from Free-Stream Pressure Measurements

As previously discussed in the Analytical Review section, the method developed for predicting Δh_v for untested liquids and conditions requires a known reference value of Δh_v. For the present study, this reference value was obtained by direct measurement of cavity pressure. However, because $K_{c,min}$ remains constant when the geometric similarity of body and cavitated region is maintained, it is possible to estimate the reference value of Δh_v without measuring cavity pressure directly. In a given flow device, two different tests are made in which the free-stream pressure requirements $(h_0 - h_v)$ to obtain geometrically similar cavitated regions are measured. These tests need not necessarily be for the same liquid, temperature, velocity, or scale; however, at least one must yield measurable thermodynamic effects of cavitation. With $K_{c,min}$ constant, equation (4) can be written as

$$\Delta h_v - \left(\frac{V_0}{V_{0,ref}}\right)^2 \left(\Delta h_v\right)_{ref} = \left(\frac{V_0}{V_{0,ref}}\right)^2 \left(h_0 - h_v\right)_{ref} - (h_0 - h_v) \tag{6}$$

Measured values from one of the two test conditions are arbitrarily chosen as the reference values in this equation. Because both Δh_v and $\left(\Delta h_v\right)_{ref}$ are unknown, an iterative procedure is required for the solution of equation (6). First a value of $\left(\Delta h_v\right)_{ref}$ is assumed. The corresponding $\left(\rho_v/\rho_l\right)_{ref}$ can be obtained from equation (1) (or the equivalent curves of fig. 3). The predicted ρ_v/ρ_l for the second test condition is calculated from equation (5) and the corresponding value of Δh_v is then obtained from equation (1) (or the equivalent curves of fig. 3). Successive calculations are made until the values of Δh_v and $\left(\Delta h_v\right)_{ref}$ satisfy equation (6). With the value of $\left(\Delta h_v\right)_{ref}$ deter-

mined, other values of Δh_v can then be predicted for other liquids, temperatures, velocities, or scales. For each predicted value of Δh_v, the corresponding free-stream pressure requirement $h_0 - h_v$ for a geometrically similar cavity can be calculated by the use of equation (6).

CONCLUDING REMARKS

Venturi cavitation data obtained with liquid hydrogen were incorporated with Freon-114 (dichlorotetrafluoroethane) data in two scaled venturis to evaluate experimental exponents used in a previously reported equation for predicting the thermodynamic effects of developed cavitation. The prediction method using the equation accounts for changes in liquid, liquid temperature, flow velocity, cavity length, and model scale. This method works well over a wide range of fluid properties and flow conditions provided that the cavitated region is uniformly developed with its leading edge at a fixed axial location, and there is local equilibrium of cavity pressure and temperature. At present, these two requirements can only be assumed for untested cases.

The use of the method requires a known value of cavity-pressure depression at one operating condition. This value for cavity-pressure depression may be obtained either by direct measurement or from two test values of inlet static pressure above vapor pressure obtained for a constant scaled cavity length, but not necessarily for the same liquid, temperature, velocity, or model scale.

Although the present study is limited to venturis, the method can be applied to the prediction of cavitation performance for pumps and inducers in a manner similar to that reported in references 2 and 3. The cavitation studies need not be conducted at particular temperatures or flow velocities because the method accounts for these changes. The development time and cost for new pumps and inducers may be reduced by conducting a relatively small number of tests using inexpensive liquids, reduced scale models, low velocities, or any combination of these. These test data may then be used to predict performance for the liquid temperature, velocity, and scale of interest.

Lewis Research Center,
National Aeronautics and Space Administration,
Cleveland, Ohio, August 15, 1968,
128-31-06-28-22.

APPENDIX - SYMBOLS

C_p	noncavitating wall pressure coefficient, $(h_x - h_0)/\left(V_0^2/2g\right)$
c_l	specific heat of liquid, Btu/(lb mass)(^oR); J/(kg)(K)
D	free-stream diameter (approach section, fig. 1), in.; cm
D_t	throat diameter (see fig. 1), in.; cm
g	acceleration due to gravity, 32.2 ft/sec^2; 9.8 m/sec^2
$h_{c,min}$	minimum measured pressure in cavitated region, ft of liquid abs; m of liquid abs
h_v	vapor pressure corresponding to free-stream liquid temperature, ft of liquid abs; m of liquid abs
Δh_v	decrease in vapor pressure corresponding to decrease in liquid temperature, ft of liquid; m of liquid
h_x	static pressure at x, ft of liquid abs; m of liquid abs
h_0	free-stream static pressure (approach section, fig. 1), ft of liquid abs; m of liquid abs
J	mechanical equivalent of heat, 778 (ft)(lb force)/Btu
$K_{c,min}$	developed cavitation parameter based on minimum cavity pressure, $(h_0 - h_{c,min})/\left(V_0^2/2g\right)$
K_v	developed cavitation parameter based on free-stream vapor pressure, $(h_0 - h_v)/\left(V_0^2/2g\right)$
k	thermal conductivity of saturated liquid, Btu/(ft)(hr)(^oR); J/(m)(sec)(K)
L	latent heat of vaporization, Btu/(lb mass); J/kg
l	approach section length (fig. 1), in.; cm
T	free-stream liquid temperature, ^oR; K
V_0	free-stream velocity (approach section, fig. 1), ft/sec; m/sec
$\mathscr{V}_l$	volume of saturated liquid, cu ft; cu m
$\mathscr{V}_v$	volume of saturated vapor, cu ft; cu m
X	axial distance from venturi inlet (see fig. 1), in.; cm
x	axial distance from minimum noncavitating pressure location (fig. 2), in.; cm

Δx	length of cavitated region, in.; cm
α	thermal diffusivity, $k/\rho_l c_l$, (sq ft)/hr; (sq m)/hr
ρ_l	saturated liquid density, (lb mass)/(cu ft); kg/(cu m)
ρ_v	saturated vapor density, (lb mass)/(cu ft); kg/(cu m)

Subscripts:

l	liquid
min	minimum
pred	predicted
ref	reference value obtained from experimental tests

Superscripts:

m, n, p	exponents, see eq. (2)

REFERENCES

1. Ball, Calvin L.; Meng, Phillip R.; and Reid, Lonnie: Cavitation Performance of 84° Helical Pump Inducer Operated in 37° and 42° R Liquid Hydrogen. NASA TM X-1360, 1967.

2. Ruggeri, Robert S.; Moore, Royce D.; and Gelder, Thomas F.: Method for Predicting Pump Cavitation Performance. Paper presented at the ICRPG Ninth Liquid Propulsion Symposium, St. Louis, Oct. 25-27, 1967.

3. Meng, Phillip R.: Change in Inducer Net Positive Suction Head Requirement with Flow Coefficient in Low Temperature Hydrogen (27.9° to 36.6° R). NASA TN D-4423, 1968.

4. Salemann, Victor: Cavitation and NPSH Requirements of Various Liquids. J. Basic Eng., vol. 81, no. 2, June 1959, pp. 167-180.

5. Spraker, W. A.: The Effects of Fluid Properties on Cavitation in Centrifugal Pumps. J. Eng. Power, vol. 87, no. 3, July 1965, pp. 309-318.

6. Stepanoff, A. J.: Cavitation Properties of Liquids. J. Eng. Power, vol. 86, no. 2, Apr. 1964, pp. 195-200.

7. Gelder, Thomas F.; Ruggeri, Robert S.; and Moore, Royce D.: Cavitation Similarity Considerations Based on Measured Pressure and Temperature Depressions in Cavitated Regions of Freon-114. NASA TN D-3509, 1966.

8. Moore, Royce D.; and Ruggeri, Robert S.: Venturi Scaling Studies on Thermodynamic Effects of Developed Cavitation of Freon-114. NASA TN D-4387, 1968.

9. Ruggeri, Robert S.; and Gelder, Thomas F.: Cavitation and Effective Liquid Tension of Nitrogen in a Tunnel Venturi. NASA TN D-2088, 1964.

10. Hord, Jesse; Edmonds, Dean K.; and Millhiser, David R.: Thermodynamic Depressions within Cavities and Cavitation Inception in Liquid Hydrogen and Liquid Nitrogen. Rep. 9705, National Bureau of Standards (NASA CR-72286), Mar. 1968.

11. Ruggeri, Robert S.; and Gelder, Thomas F.: Effects of Air Content and Water Purity on Liquid Tension at Incipient Cavitation in Venturi Flow. NASA TN D-1459, 1963.

12. Wylie, Clarence R., Jr.: Advanced Engineering Mathematics. Second Ed., McGraw-Hill Book Co., Inc., 1960, pp. 175-191.

NATIONAL AERONAUTICS AND SPACE ADMINISTRATION
WASHINGTON, D. C. 20546

OFFICIAL BUSINESS

FIRST CLASS MAIL

POSTAGE AND FEES PAID
NATIONAL AERONAUTICS AND
SPACE ADMINISTRATION

POSTMASTER: If Undeliverable (Section 158
Postal Manual) Do Not Return

"The aeronautical and space activities of the United States shall be conducted so as to contribute . . . to the expansion of human knowledge of phenomena in the atmosphere and space. The Administration shall provide for the widest practicable and appropriate dissemination of information concerning its activities and the results thereof."

—NATIONAL AERONAUTICS AND SPACE ACT OF 1958

NASA SCIENTIFIC AND TECHNICAL PUBLICATIONS

TECHNICAL REPORTS: Scientific and technical information considered important, complete, and a lasting contribution to existing knowledge.

TECHNICAL NOTES: Information less broad in scope but nevertheless of importance as a contribution to existing knowledge.

TECHNICAL MEMORANDUMS: Information receiving limited distribution because of preliminary data, security classification, or other reasons.

CONTRACTOR REPORTS: Scientific and technical information generated under a NASA contract or grant and considered an important contribution to existing knowledge.

TECHNICAL TRANSLATIONS: Information published in a foreign language considered to merit NASA distribution in English.

SPECIAL PUBLICATIONS: Information derived from or of value to NASA activities. Publications include conference proceedings, monographs, data compilations, handbooks, sourcebooks, and special bibliographies.

TECHNOLOGY UTILIZATION PUBLICATIONS: Information on technology used by NASA that may be of particular interest in commercial and other non-aerospace applications. Publications include Tech Briefs, Technology Utilization Reports and Notes, and Technology Surveys.

Details on the availability of these publications may be obtained from:

SCIENTIFIC AND TECHNICAL INFORMATION DIVISION

NATIONAL AERONAUTICS AND SPACE ADMINISTRATION

Washington, D.C. 20546